678

PROPOSAL TO STUDY THE SPIN DEPENDENCE IN INCLUSIVE π° AND DIRECT GAMMA PRODUCTION AT HIGH P_T WITH THE POLARIZED PROTON BEAM FACILITY AT FERMILAB

by

D. Hill, H. Spinka, R. Stanek, K. Toshioka, D. Underwood, and A. Yokosawa
Argonne National Laboratory, Argonne, Illinois

Y. Hemmi, K. Imai, R. Kikuchi, K. Miyake, T. Nakamura,
K. Nishimura and N. Tamura
Kyoto University, Kyoto, Japan

H. Azaïez, K. Kuroda, A. Michalowicz, D. Perret-Gallix
LAPP, Annecy, France

G. Shapiro
Lawrence Berkeley Laboraotry
University of California, Berkeley, California

D. H. Miller and C. LeRoy
Northwestern University, Evanston, Illinois

M. Corcoran, H. E. Miettinen, T. A. Mulera, G. S. Mutchler,
G. C. Phillips and J. B. Roberts
Rice University, Houston, Texas

J. Bistrisky, A. DeLesquen, F. Lehar, and L. Van Rossum
Saclay, France

V. Apokin, Y. Matulenko, A. Meschanin, S. Nurushev,
V. Solovyanov and A. Vasilyev
Serpukhov, USSR

R. Birsa, F. Bradamante, S. Dalla Torre-Colautti, M. Giorgi, L. Lanceri,
A. Martin, P. Moras, A. Penzo, P. Schiavon and A. Villari
INFN, Sezione di Trieste, Trieste, Italy

January 25, 1981

Scientific Spokesman:
K. Kuroda
LAPP, Annecy, France
Telephone: (50)-23-32-45

ABSTRACT

We propose to measure the single-spin asymmetry parameter A_N in inclusive π^o production and direct-γ production at high p_T using the polarized proton-beam facility at Fermilab. In addition, we propose to measure the double-spin asymmetry parameter A_{LL} in inclusive π^o production using a polarized proton target. The measurement of A_{LL} will be extended to direct-γ production when improved target materials become available.

I. INTRODUCTION

Investigation of the substructure of hadrons and the behavior of hadronic constituents is presently among the most active areas of high energy physics. Recent data on deep-inelastic ep scattering [1)2)] are most directly interpreted as evidence that quarks at large-X have high probability for retaining the helicity of the parent proton. Since high-p_T hadron or photon production results predominantly from the hard scattering of hadronic constituents it is reasonable to expect that spin dependence in these fundamental subprocesses can be further investigated using polarized protons [3)4)5)].

We propose to study spin dependence in the reactions

$$p + p \to \pi^o + \text{anything}, \quad \text{and} \qquad (1)$$

$$p + p \to \gamma + \text{anything} \qquad (2)$$

with emphasis on the high-p_T region. The quantities to be measured are the single-spin asymmetries

$$A_N = \frac{Ed^3\sigma(\uparrow)/dp^3 - Ed^3\sigma(\downarrow)/dp^3}{Ed^3\sigma(\uparrow)/dp^3 + Ed^3\sigma(\downarrow)/dp^3} \qquad (3)$$

for both reactions (1) and (2) with a transversely polarized proton beam and liquid hydrogen (H_2) target. In addition we propose to measure the double-spin asymmetry in reaction (1)

$$A_{LL} = \frac{Ed^3\sigma(++)/dp^3 - Ed^3\sigma(+-)/dp^3}{Ed^3\sigma(++)/dp^3 + Ed^3\sigma(+-)/dp^3} \qquad (4)$$

where ++(+-) indicate parallel (antiparallel) helicities for longitudinally polarized beam and target protons. This measurement requires replacement of the liquid H_2 target by a polarized proton target (PPT).

II. PHYSICS MOTIVATION

The single-spin asymmetries in reactions (1) and (2) are expected to be close to zero in current QCD theory even with higher order corrections ($A_N \simeq O(m_q/\sqrt{s})$ where m_q is the mass of the light quark). Nevertheless, large asymmetries in inclusive π^o production have been observed at the CERN PS[6] for $p_{in} = 24$ GeV/c, $X_F \simeq 0$, and $1.0 < p_T < 2.5$ GeV/c. Although this kinematic region may be too low to contradict directly the validity of the constituent model based on QCD these results provide strong motivation for extending similar measurements to regions of higher p_{in} and p_T. The high-intensity polarized-proton facility to be constructed at Fermilab[7] can usefully cover the p_T region to 4-5 GeV/c at $p_{in} = 300$ GeV/c for both reaction (1) and (2). If large asymmetries are observed at such large p_T they would present a serious challenge to the attractive model of hard scattering and perturbative QCD.

The QCD Compton effect, gluon + quark → gamma + quark, is expected to be the dominant mechanism for direct-γ production at large p_T. In contrast to the π^o which represents only a fragment of the scattered constituent the γ itself participates directly in the hard-scattering process. As a direct consequence the ratio γ/π^o should increase with increasing p_T; this prediction has recently been confirmed in several different experiments[8)9)10)]. Thus, direct-γ production provides a particularly clean process for studying the dynamics of hadronic constituents without the complexities of quark fragmentation. We emphasize that on the experimental side the use of a polarized beam on a liquid H_2 target provides a particularly clean technique for studying single-spin asymmetries without the complexity of polarized targets and the unavoidable background from production on unpolarized constituents therein.

Although important qualitative features may be deduced from single-spin asymmetry measurements, the study of double-spin asymmetries can provide quantitative insight into the spin properties of gluons which are not accessible to deep-inelastic ep scattering experiments. The double-spin asymmetry A_{LL} in inclusive π^o production has been estimated by several authors; their results are shown in Fig. 6. Curve (a) was obtained by Babcock et al.[3] using a hard-scattering model based on QCD perturbation theory; although the predicted asymmetry is small it has a definite positive sign. Cheng and Fischbach[5)] predict a much larger asymmetry using the effective-gluon model (E-G); Sivers et al.[11)] find zero asymmetry in the constituent interchange model (CIM). The large differences are a consequence of the different spin dependences assumed in the fundamental subprocesses for these models; the present experient will be sufficiently sensitive to discriminate among these models.

The double-spin asymmetry for direct-γ production has recently been estimated by Hidaka[12)] assuming QCD Compton and $q\bar{q}$ annihilation as dominant subprocesses. These same assumptions successfully describe available data for the unpolarized cross sections. His results suggest significant asymmetries at large X_T ($\simeq 5\%$ at $X_F \simeq 0$ and $X_T \simeq 0.5$). Because of the polarization dilution in available polarized proton targets A_{LL} cannot yet be measured with adequate precision; however, targets of sufficient spin purity are under development at Saclay and CERN. Because of the importance of direct-γ production as a hadronic probe we propose to extend the double-spin measurements to this final state when improved target materials become available.

III. EXPERIMENTAL METHODS

a) Experimental Arrangement

A schematic view of the experimental arrangement is shown in Fig.1. The polarized proton beam to be constructed in the M2 beam line[7)] enters from the left. Trajectories of individual beam particles are defined by hodoscopes H_1 and H_2; these are separated by 20 meters and have spatial resolutions of 1.5 mm in both the x and y directions. For single-spin measurements a liquid H_2 target 100 cm long will be used with the proton beam transversely polarized. For the double-spin asymmetry measurements the longitudinally polarized proton beam will be incident on a longitudinally polarized proton target. The proposed snake system will allow the beam polarization to be flipped from spill to spill with no important change in beam geometry.

Gammas produced by the interaction of protons on either target are detected in the two Pb-glass spectrometers G_1 and G_2. At p_{in} = 300 GeV/c the spectrometers are placed 12 m downstream of the target and centered around Θ = 80 mrad which corresponds to X_F = 0. The azimuthal angle subtended by each spectrometer is $\pm 22.5^\circ$ with respect to the horizontal plane.

The scintillation hodoscopes H_3 and H_4, immediately in front of the Pb-glass spectrometers, are constructed in three planes for segmentation in the X, Y, and U directions; these have spatial resolutions of 4 cm and serve to localize charged particles which accompany γ's. To improve background identification in direct-γ production each Pb-glass spectrometer is provided with a guard counter G_1' and G_2'. These coarse-grained Cerenkov shower counters ensure identification of π^o and η^o decays in which only one γ falls within the fiducial area of a Pb-glass spectrometer.

The acceptance of the detector in X_F-p_T space is shown in Fig. 2 for p_{in} = 300 GeV/c.

b. Gamma Spectrometers

The two gamma spectrometers comprise the major part of the detector. Each consists of 372 Pb-glass cells (3.8x3.8x45 cm) stacked to form a trapezoidal array as shown in Fig. 3. The Cerenkov light is collected by a photomultiplier at the rear of each cell. The detector elements and the design of the associated electronic system will be similar to those developed by the IHEP-IFSN-LAPP Collaboration for the GAMS 4000 spectrometer[13)] at CERN. The principal characteristics of this spectrometer are listed in Table 1.

The remarkable spatial resolution of the GAMS spectrometer (±1 mm at 200 GeV) results from an optimal choice of transverse dimension 2Δ of the Pb-glass cells[14)]. By choosing Δ just slightly smaller than the effective half-width (2 cm for Pb-glass of type F-8) of an electromagnetic shower it spreads over only a few cells to form a cluster. A fit to the energy deposition pattern in the cluster provides the position coordinates for the incident γ. The ability to resolve the merged clusters produced by two close γ's is particularly important for efficient identification of direct-γ's in a background of π^o decays. The IHEP group has found experimentally[15)] that pairs of γ's from π^o decay can be discriminated from single γ's for transverse separations greater than 2.5 cm even when both γ's fall within the same cell of the spectrometer.

Geometric efficiencies for π^o detection have been studied using Monte Carlo simulation; results are shown in Fig. 4 for a kinematic region around X_F = 0. With increasing p_T the probability for detecting both γ's from a π^o decay (solid circles) asymptotically approaches the

25% azimuthal angle subtended by the spectrometers ($2x45^o$). At lower p_T the efficiency decreases as the probability for one of the γ's to miss a spectrometer increases. For $X_F = 0$ the probability that only a single γ falls within the detector acceptance (triangle points) decreases rapidly with increasing p_T. For $X_F \neq 0$ the π^o angle varies rapidly with p_T; this results in a maximum near $p_T = 4$ GeV/c for the probability that a single γ falls within the detector acceptance. The probability that both γ's from a π^o decay fall within a single cell (open circles) is almost negligible for $p_T < 7$ GeV/c. Even so, many of these events will be resolved since the transverse separation of the two γ's will be larger than the discrimination limit of 2.5 cm.

To accommodate high event rates the integrated charge in each cell is digitized with its own ADC. Pedestal subtraction and energy normalization are performed automatically by a fast processor. Relative gains (PM + ADC) will be monitored under microprocessor control with an LED system between spills to achieve a long-term stability better than 1%. The energy resolution has been measured for a spectrometer of this type; at full width half-maximum (FWHM) it is

$$\Delta E/E = 0.025 + 0.13/\sqrt{E}(\mathrm{GeV})$$

giving ± 2.5% at 25 GeV. Linearity has been studied with electrons from 1-4 GeV by the EHS group at CERN and from 1.8-40 GeV by the GAMS group at IHEP. No deviation larger than 1% was observed.

Energies and coordinates (using the method of moments) will be evaluated on-line. This provides the possibility for imposing event selection criteria if necessary before recording data on tape. With reasonable estimates for processing times we conclude that as many as 500 events/sec can be recorded even with large multiplicities.

c. Identification of π^o Events

Fast discriminators sample the integrated charge in each cell. Thresholds are adjusted so that the detector is triggered when an energy greater than 10 GeV is deposited in any cell. This allows efficient detection of π^o's emitted near $X_F \simeq 0$ and $p_T < 2.0$ GeV/c. If rates are too high the discriminator thresholds can be increased or the hodoscopes H_3 and H_4 can be used to reject clusters associated with charged particles. It is apparent, however, that event reject is preferably executed off-line after careful study so that no bias is introduced in the inclusive final states.

To obtain a 'clean' sample of π^o events all data must be subjected to extensive off-line analysis. Backgrounds due to improperly paired γ's will be estimated using Monte Carlo simulation with reconstructed π^o's as input. Contamination of the final sample by π^o's from decay of inclusively produced η^o's, ω^o's, and K_s^o's can be reasonably estimated from available measurements and models which relate charged and neutral production. This contamination will be small at high p_T.

d. Identification of Direct-γ Events

The problems involved in identification of direct-γ 's in a background of π^o decays have recently been addressed with considerable success by several groups[8)9)10)]. Background arises from

i) The decays $\pi^o \to \gamma\gamma$ and $\eta^o \to \gamma\gamma$ in which one γ misses a spectrometer, is below threshold for detection, or converts in the target; or the two γ's are too closely spaced to be geometrially resolved; and

ii) Neutral hadrons such as n, $\bar{n}$, or K_L^o which interact in the Pb-glass and simulate a single shower.

We propose to surround the Pb-glass spectrometers with gaurd counters to detect γ's which otherwise would be lost. With Monte Carlo simulation we find that a lateral thickness of 30 cm is enough to detect 97% of these associated γ's arising from decay of π^o's emitted near $X_F = 0$ with $p_T \simeq 5$ GeV/c. Because of the large volume (0.5 m^3) and complex shape of the gaurd counters we propose to use a water solution of heavy elements (for example ZnI, with $\rho \simeq 2.8$, and R.L. $\simeq 4.2$ cm) as recently developed at KEK[16)]. The direct measurement of this important background will result in significant improvement of the final error compared with the alternative of subtracting background with Monte Carlo simulation. The background from unresolved π^o decays is very small. Less than 0.3% of all π^odecays falling within the detector acceptance are unresolved for $p_T \simeq 6$ GeV/c; for $\gamma/\pi^o \simeq 0.1$ this represents only a 3% background for direct-γ's. The background from conversions in the target can be reliably estimated from the reconstructed π^o events.

The neutral hadron contribution to background will be measured in a separate run using the method of Cox et al.[10)]. Ten radiation lengths of Pb will be inserted in the space between the hodoscopes H_3 and H_4 and the Pb-glass spectrometers. The γ flux is largely degraded while the neutral hadronic component is attenuated only 30% due to interactions in the Pb. This background varies from 10 to 40% depending on the kinematic region and therefore must be subtracted separately in each X_F and p_T interval.

Measurement of single-spin asymmetries will be carried out simultaneously for the inclusive π^o's and direct-γ's.

IV. RATE AND ERROR ESTIMATES

Rates for π^o production have been estimated with the following assumptions:

p_{in} = 300 GeV/c
Beam intensity = $3x10^7$/spill with 1 spill/60 sec and
polarization P_b = 0.5
Geometrical efficiency for π^o detection = 0.25
Liquid H_2 target 100 cm long for A_N measurements
Propanediol polarized proton target 15 cm long with
polarization P_t = 0.8 for A_{LL} measurements.

The invariant cross section was calculated with the parameterization of Büsser et al.[17)]

$$f = E \frac{d^3\sigma}{d^3p} = C \ p_T^{-n} \ e^{-b \ X_T} \qquad (5)$$

where $C = 14.2x10^{-27}$ cm^2/GeV^2, n = 8.6, and b = 12.5. The results are given in Table 2 for an integrated beam intensity of $1.6x10^{12}$ polarized protons corresponding to 1000 running time.

Statistical Errors

For a transversely polarized the observed single-spin asymmetry is given by

$$\varepsilon = \frac{(N_R + N_{Rb}) - (N_L + N_{Lb})}{(N_R + N_{Rb}) + (N_L + N_{Lb})} \simeq \frac{N_R - N_L}{N_{total}}$$

where $N_R(N_L)$ is the right (left) signal and $N_{Rb}(N_{Lb})$ is the right (left) background with $N_{Rb} \simeq N_{Lb}$. Then the observed asymmetry is related to

A_N through

$$\varepsilon = \frac{N_R + N_L}{N_{total}} \cdot \frac{N_R - N_L}{N_R + N_L} = \frac{1}{\chi} P_b A_N$$

where $\chi = (N_{total})/(N_R + N_L)$. The statistical error in A_N may then be approximated

$$\Delta A_N \simeq \frac{\chi}{P_b} \Delta\varepsilon$$

where $\Delta\varepsilon \simeq 1/\sqrt{(N_{total})}$. In this case the backgrounds N_{Rb} and N_{Lb} result largely from pairs of uncorrelated γ's which fall within the π^o acceptance criteria. This background can be estimated from the 2γ effective-mass distributions. With $\chi = 1.1$ as a reasonable estimate we obtain the errors ΔA_N given in Table 2.

A similar estimate has been made for ΔA_N in direct-γ production. In this case it was assumed that the ratio γ/π^o varied from 0.08 at $p_T = 3$ GeV/c to 0.2 at $p_T = 5$ GeV/c[10]. The backgrounds N_{Rb} and N_{Lb} result from the sources discussed in Sec. IIId where procedures for estimating their contributions are described. With the assumption $\chi \simeq 1.1$ we obtain the estimated statistical errors given in Table 2.

The double-spin asymmetry measurements require both polarized beam and target. The statistical error may be approximated

$$\Delta A_{LL} \simeq \frac{\chi\,\alpha}{P_b P_t} \Delta\varepsilon$$

here the 'polarization dilution factor' α reflects production on unpolarized target constituents, principally carbon and oxygen. This factor depends not only on the target material but also on the kinematic conditions, particularly p_T. To estimate ΔA_{LL} we assumed that α varies monotonically from 10-20 as p_T increases from 2-5 GeV/c. Accurate evaluation of α requires a detailed study of the A-dependence of the reaction through the relevant kinematic region.* With the assumption that $\chi \simeq 1.5$ for the double-spin asymmetry we obtain the errors ΔA_{LL} given in Table 2.

---

*It should be noted that the effect of the dilution factor is frequently overestimated. The statistical error in the asymmetry depends, in fact, only on $\sqrt{\alpha}$ since the error in the asymmetry $\Delta\varepsilon \simeq 1/\sqrt{N_{total}} \simeq 1/\sqrt{\chi\alpha(N_R + N_L)}$.

Systematic Errors

The systematic errors divide roughly into multiplicative and additive. Uncertainties in target and beam polarizations are multiplicative errors. Target polarization can be measured to ±3% with the principal uncertainty in calibration of the nuclear magnetic resonance system which uses the thermal equilibrium signal. It is estimated that beam polarization can be calculated to ±3% from the beam optics. Neverltheless, we propose to measure this independently with a high-rate polarimeter based on elastic scattering in the Coulomb-nuclear interference region[18)]; this will provide an accuracy of ±5% even for runs as short as a few hours.

An additional multiplicative error in ΔA_{LL} arises from the uncertainty in target dilution α. This can be estimated with good accuracy from measurements of single- and double-spin asymmetries using liquid H_2 and a polarized proton target with identical detector conditions.

Additive errors which may introduce a spurious asymmetry in the data can arise from

i) changes in beam geometry with reversal of beam polarization
ii) misalignment of detector components
iii) changes in gain of spectrometer elements.

Geometric sources of error associated with either the beam or detector can be accurately controlled through frequent cross-checks of counting rates with different spin-spin and spin-detector (right or left) combinations. The gain stability of the Pb-glass counters will be controlled to an accuracy better than 1%. With frequent reversals of beam polarization long-term variations in gain will average away.

Comparison with Theory

The statistical errors estimated in Table 2 have been superimposed on relevant theoretical predictions in Fig. 5 and 6. Fig. 5 shows ΔA_N for π^o and direct-γ production; the QCD prediction is near zero for each. We show also the experimental results for π^o production at 24 GeV/c[6)]. The greatly improved accuracy even at much larger p_T expected in the present experiment results directly from the use of a polarized beam and liquid H_2 target rather than an unpolarized beam and a polarized proton target with its large dilution factor. Up to 5 GeV/c, where QCD predictions become meaningful, asymmetries larger than 5% in inclusive π^o production and larger than 15% in direct-γ production will be reliably detected. It may be noted that the integrated luminosity ($\simeq 5\text{x}10^{37}/\text{cm}^2$)

is comparable to that of the most extensive ISR experiments so that our measurements of cross sections for direct-γ production on H_2 will provide important new data at these energies.

Fig. 6 shows ΔA_{LL} superimposed on relavant predictions for inclusive π^o production. A significant asymmetry in the region $p_T < 3$ GeV/c would provide strong evidence against a scalar gluon for which no asymmetry is expected. Consequently, this experiment will not only discriminate among different models but it may also provide important insight into the gluon spin structure.

The double-spin asymmetry in direct-γ production cannot yet be measured with useful accuracy because of the large dilution factor α in available polarized targets. However, we place high priority on this part of the program when improved target materials reach practical use.

V. RUN PLAN AND BEAM REQUIREMENTS

As discussed earlier, the design of the gamma spectrometers has profited greatly from the long experience of the GAMS group. In addition, members of our Collaboration are currently involved in an experiment at Serpukhov which utilizes a gamma spectrometer with 500 elements identical to those proposed here; 250 have already been fabricated and are in use. These elements will become available and form the major part of the gamma spectrometers; the entire detector could be completed for early measurements in the polarized proton beam facility at Fermilab.

Before the start of data-taking with a liquid H_2 target we request 200 hours of unpolarized proton beam for checking out the entire system. A portion of this time would be run at high intensity, 6×10^8 p/spill, in order to measure the cross sections for inclusive π^o and direct-γ production with good precision. This preliminary run will provide a precise calibration of the apparatus for the purpose of detecting direct-γ's with high efficiency.

Single-spin asymmetries for both reactions will be measured simultaneously. To achieve this we request 1200 hours of polarized proton beam; this includes 200 hours for measurement of backgrounds induced by neutral hadrons. In addition, we request 1200 hours of polarized proton beam to measure the double-spin asymmetry in inclusive π^o production with the same detector conditions and the liquid H_2 target replaced by a polarized proton target.

The total request is thus:

200 hours of unpolarized proton beam, and
2400 hours ($\simeq$ 3 months) of polarized proton beam.

Because our detector is particularly compact and simple it should be compatible with detectors designed for other measurements in the polarized proton beam facility. In this case all or part of the time requested can be used simultaneously for additional measurements.

A measurement of the double-spin asymmetry in direct-γ production represents a natural extension of this program. This requires improved target materials such a LiD or NH_3 and possibly an elaboration of the detector to complete the 2π azimuthal geometry. If the new target material is available at run time this measurement will be carried out simultaneously with the measurement of A_{LL} in inclusive π^o production without the need for additional beam time.

REFERENCES

1) M.J. Alguard et al.,Phys.Rev. Lett. 37 1258,1261(1976)and 41 70(1976).

2) V.W.Hughes,Talk given at the InternationalSymposium on High Energy Physics with Polarized Beam and Targts,Lausanne, Switzerland,25 sep - 1 oct 1980.

3) J.Babcock,E.Monsay and D.Sivers,Phys.Rev.Lett.40 1161(1978) and Phys.Rev. D19 1483(1979)

4) J.Ranft and G.Ranft,Phys.Lett.77B 309(1978)

5) H.Cheng and E.Fischback,Phys.Rev. D19 860(1979)

6) J.Antille et al.,Phys. Lett. 94B 523(1980)

7) ANL-LAPP-LBL-RICE-TRIESTE Collaboration Fermilab proposal N°581

8) M.Diakonou et al.,Preprint CERN-EP/80-02 15 Jan.1980

9) A.L.S.Angelis et al.,Preprint CERN-EP/80-68 19 May 1980

10) B.Cox,Proc. 1979 International Symposium on Lepton and Photon Interactions at High Energies,Fermilab,Batavia,p602

11) D.Sivers,S.Brodsky and R.Blankenbeckler,Physics Reports 23C 1 (1976)

12) K.Hidaka,Preprint Westfield College,1980 and Proc. of the XV th Rencontre de Moriond,Savoie,France,March 1980

13) IHEP-IISN-LAPP Collaboration, SPS proposal SPSC/P110

14) G.A.Akopdjanov et al.,Nuc.Instr.&Method 140 441 (1977)

15) V.A.Davidov et al., Nuc. Instr. Methods 145 267(1977)

16) T.Kusumegi,Private communication

17) F.W.Büsser et al.,Nuc.Phys. B106 1(1976)

18) K.Kuroda A.Penzo and V.Soloviancv,EP internal report 79-1 Jan.1979

19) V. Bouffard et al. to be published in Journal de Physique.

TABLE 1

Parameters and characteristics	
- Lead-glass cell dimensions	38×38×450 mm^3
- Type of glass	F-8
- Total number of cells	744
- Working area and weight of the spectrometer	0.8 m^2, 2.5 t
- Photomultiplier	FEU-84-3
- Accuracy in measuring photon coordinate	
at 25 GeV	± 2 mm
at 200 GeV	± 1 mm
- Photon energy resolution	
at 25 GeV	± 2.5 %
at 200 GeV	± 1.5 %
- Mass resolution for decaying particles	a few %
- Time resolution	40 nsec gate

TABLE 2

p_T (GeV/c)	X_T	ΔX_F	Δp_T	n	ΔA_N %	n	α	ΔA_{LL} %
2	0.17	0.1	0.5	———	———	4.4×10^6	10	± 0.39
3	0.25	0.125	1.0	7.8×10^5	±0.22	1.2×10^5	13	± 2.8
4	0.34	0.15	1.0	2.8×10^4	±1.3	4.1×10^3	17	±16.9
5	0.42	0.20	1.0	1.9×10^3	±4.8	2.8×10^2	20	±69.0
6	0.51	0.30	1.0	2.1×10^2	±14.0	3.1×10^1	—	———

TABLE 3

p_T (GeV/c)	X_T	ΔX_F	Δp_T	$\gamma/\pi°$	n	ΔA_N %
3	0.25	0.125	1.0	0.08	6.3×10^4	±1.0
4	0.34	0.15	1.0	0.12	3.3×10^3	±4.4
5	0.42	0.20	1.0	0.15	2.9×10^2	±14.5
6	0.51	0.30	1.0	0.19	3.9×10^1	±39.0

For the reason of simplicity we present here $p_\perp$ corresponding to the average cross section of the (non-symmetric) binning. The weighted p_T is about 0.15 GeV/c less than the indicated one but the correction to be introduced in the cross section is less than the ambiguity on the experimental values at large $p_\perp$ region.

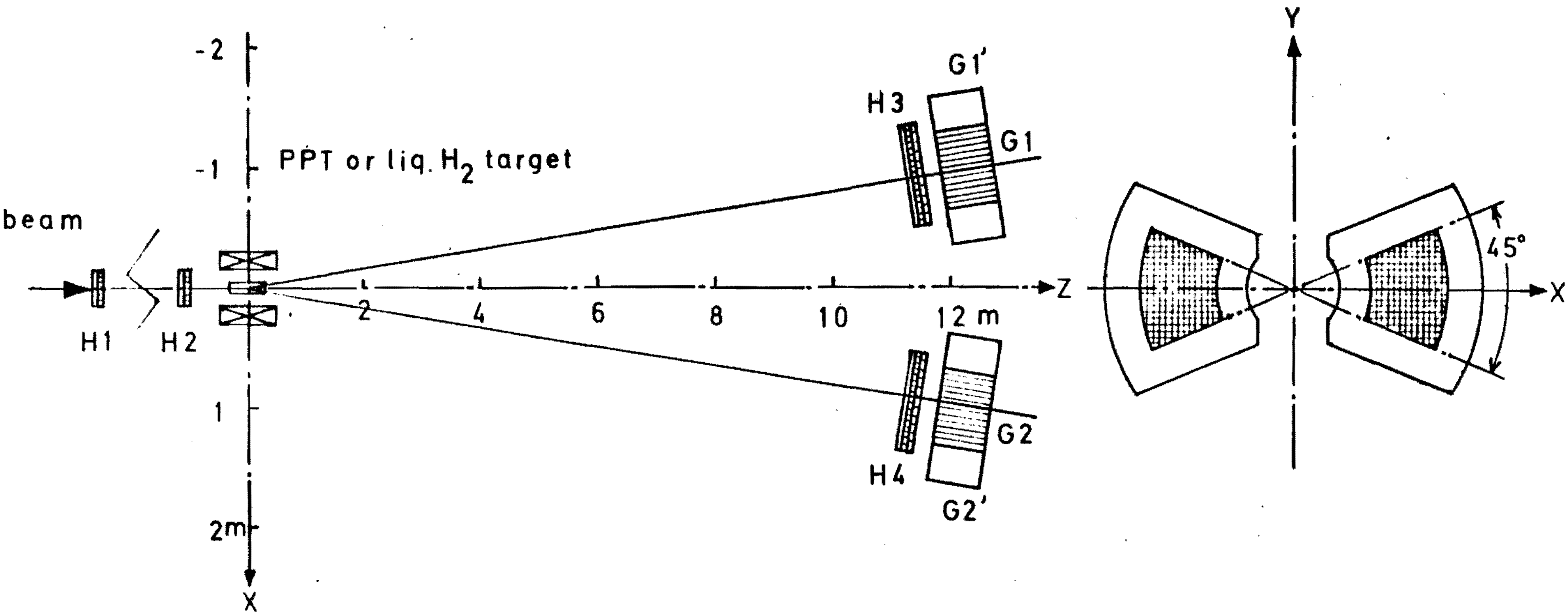
beam
H1
H2
PPT or liq. H_2 target
-2
-1
1
2m
X
2
4
6
8
10
12 m
Z
H3
G1'
G1
H4
G2
G2'
Y
X
45°

Fig.1

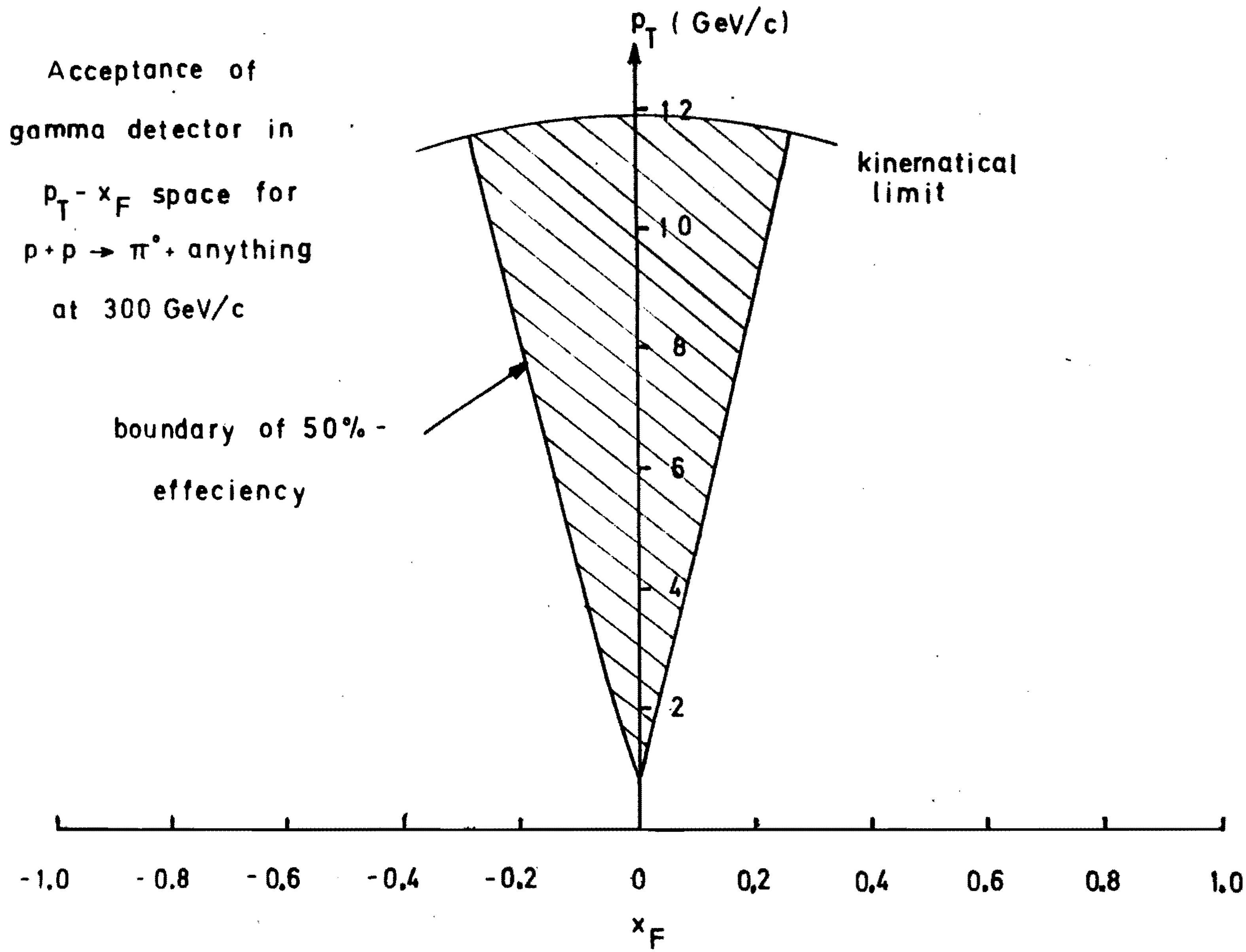

Acceptance of gamma detector in $p_T - x_F$ space for $p + p \to \pi^\circ +$ anything at 300 GeV/c
p_T (GeV/c)
12
10
8
6
4
2
kinematical limit
boundary of 50% - effeciency
-1.0
- 0.8
- 0.6
- 0.4
- 0.2
0
0.2
0.4
0.6
0.8
1.0
x_F

Fig. 2

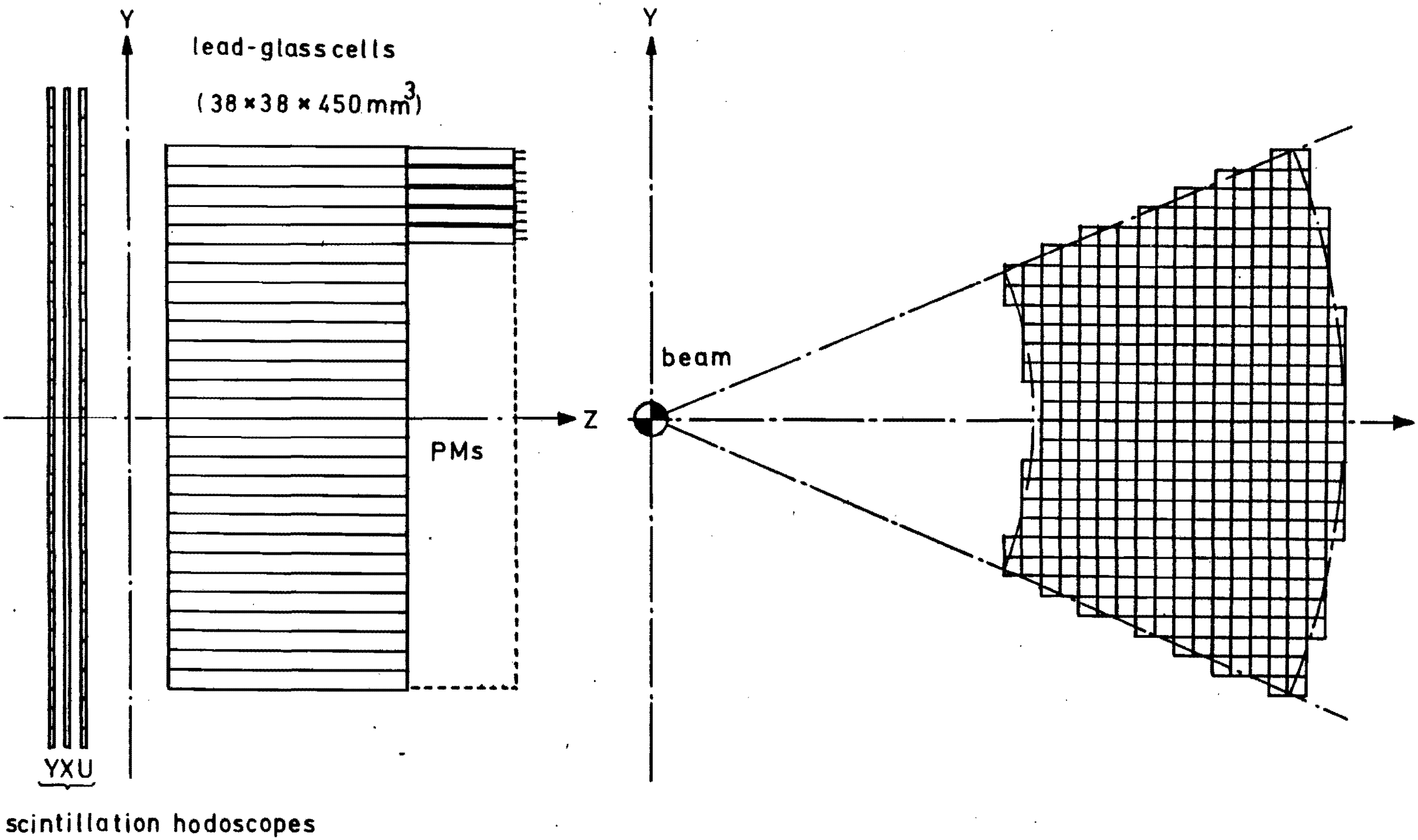
Y
lead-glass cells
(38 × 38 × 450 mm³)
Z
PMs
YXU
scintillation hodoscopes
Y
beam
X

Fig. 3

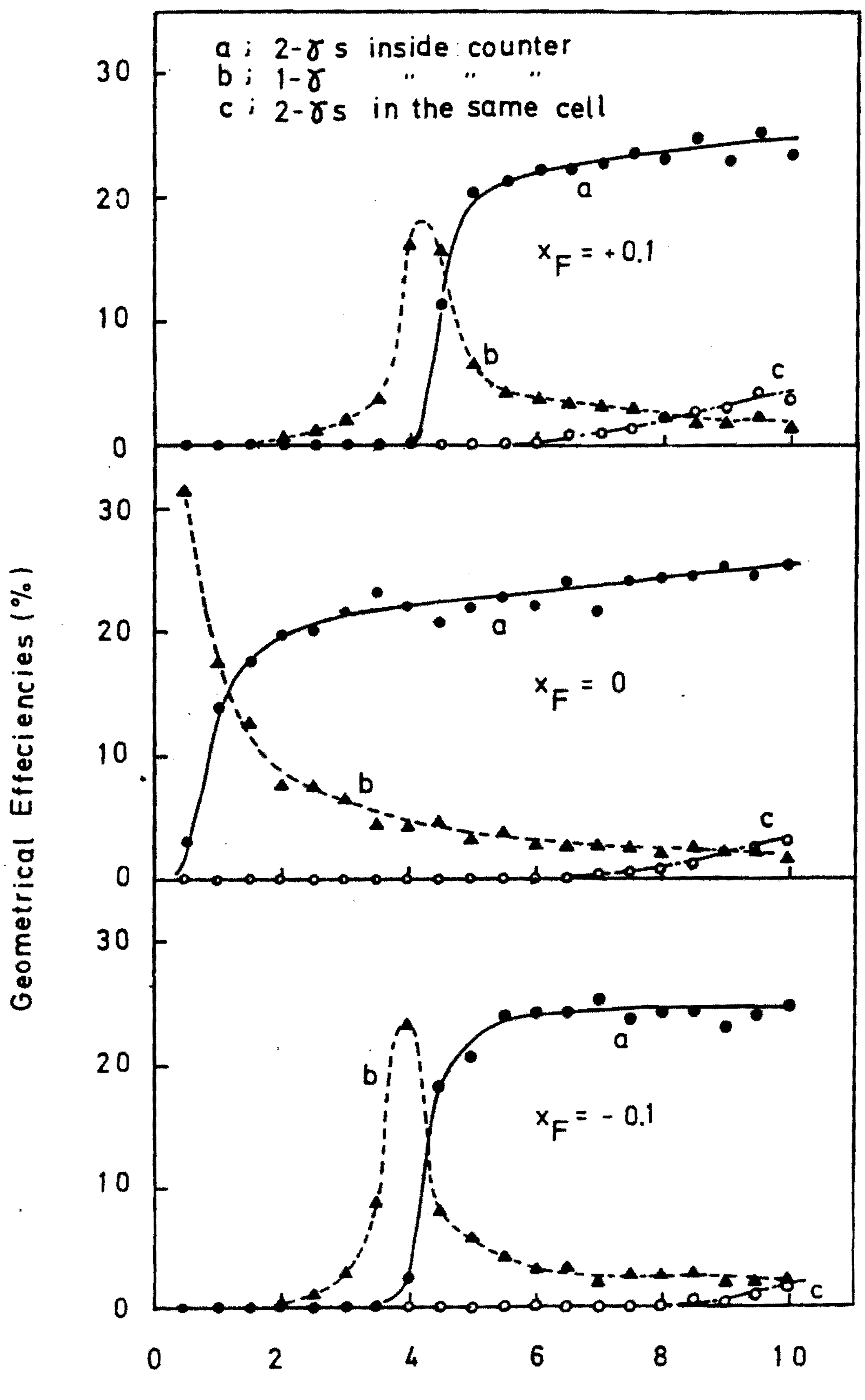
a ; 2-γ s inside counter
b ; 1-γ " " "
c ; 2-γ s in the same cell
x_F = +0.1
x_F = 0
x_F = - 0.1
a
b
c
Geometrical Effeciencies (%)
p_T (GeV/c)
0
10
20
30
0
2
4
6
8
10

Fig. 4

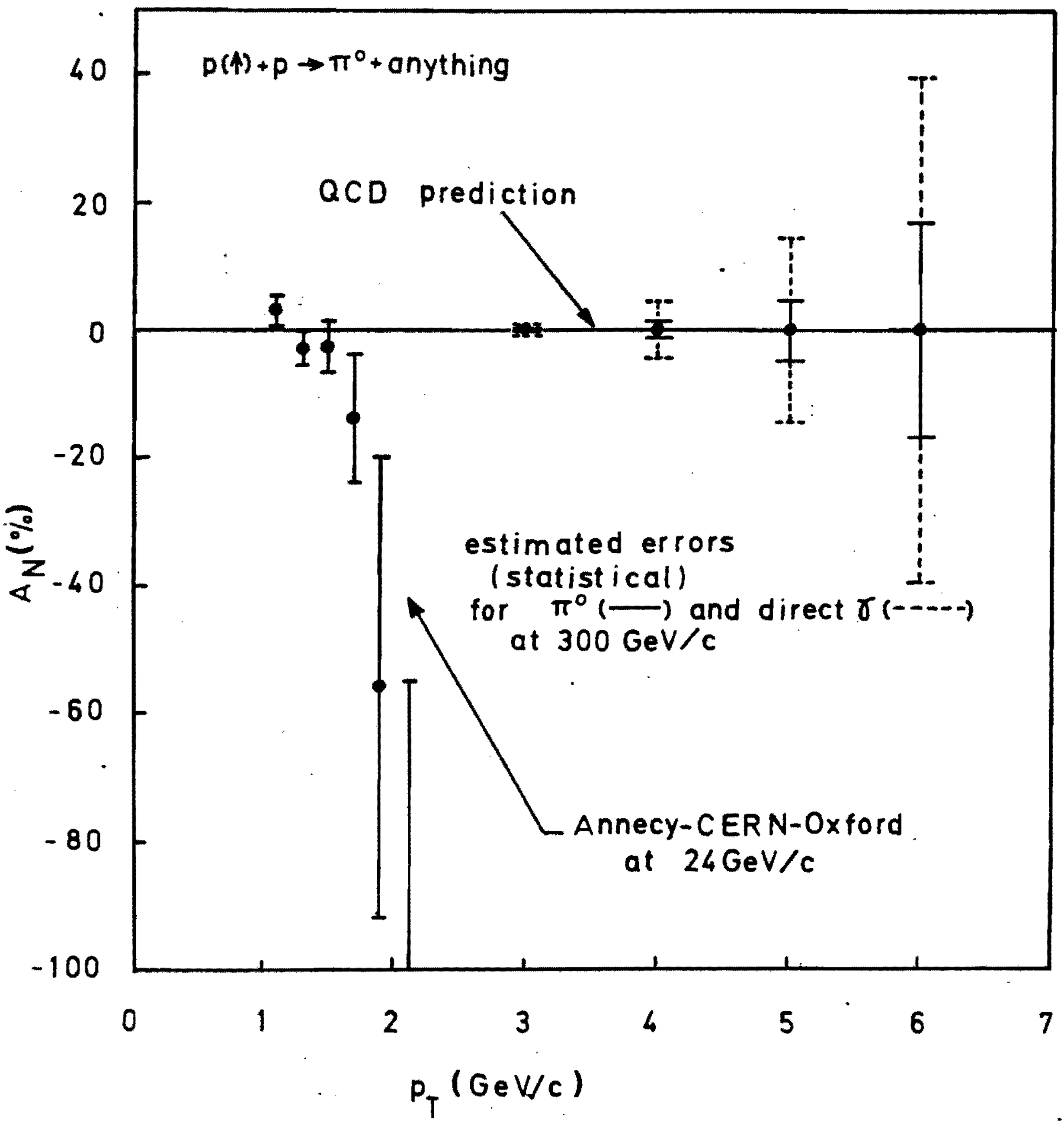

p(↑)+p → π° + anything
QCD prediction
estimated errors
(statistical)
for π° (——) and direct γ (-----)
at 300 GeV/c
Annecy-CERN-Oxford
at 24GeV/c
A_N(%)
40
20
0
-20
-40
-60
-80
-100
0
1
2
3
4
5
6
7
p_T (GeV/c)

Fig. 5

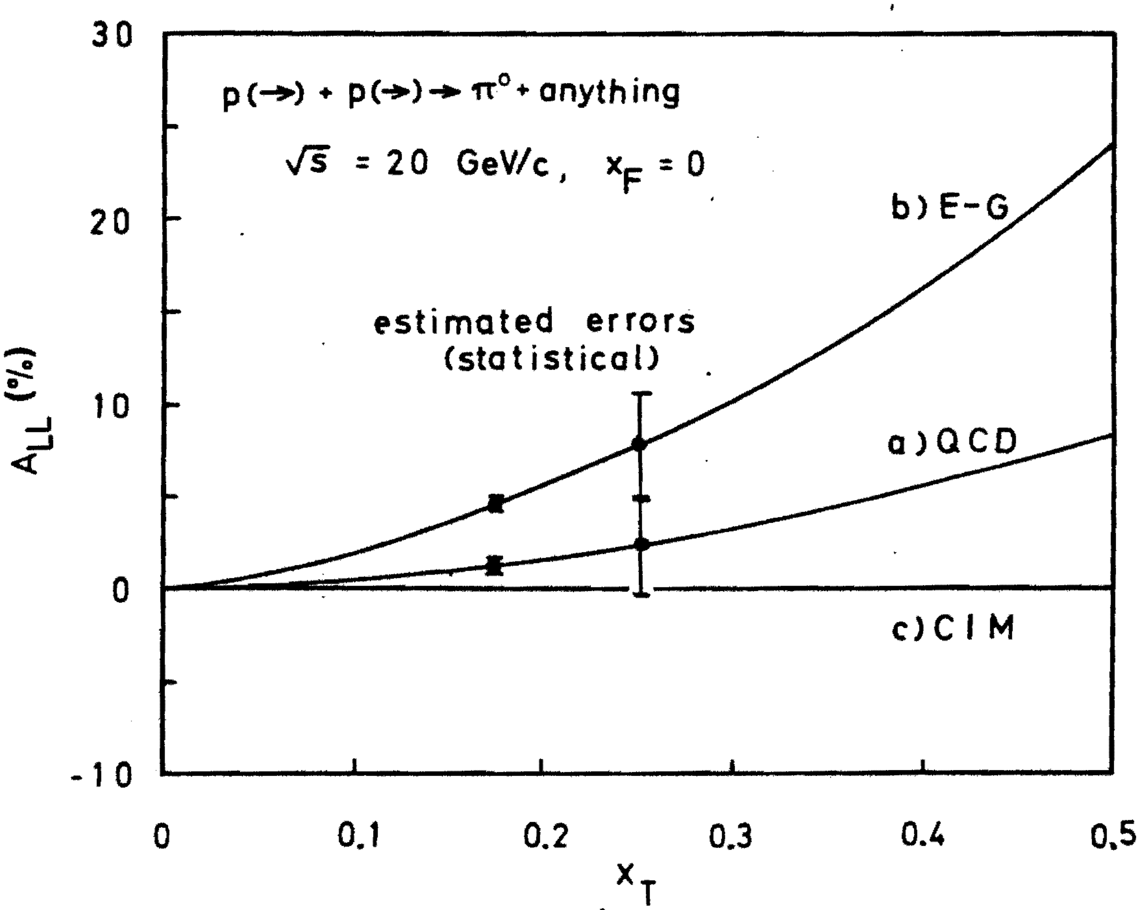
30
20
10
0
-10
0
0.1
0.2
0.3
0.4
0.5
A_{LL} (%)
x_T
$p(\rightarrow) + p(\rightarrow) \rightarrow \pi^0 +$ anything
$\sqrt{s}$ = 20 GeV/c, $x_F = 0$
b) E-G
estimated errors
(statistical)
a) QCD
c) CIM

Fig. 6

Proposal to Study the Spin Dependence in Inclusive π^0 and Direct-Gamma Production at High $p_\perp$ with the Polarized Proton Beam Facility at Fermilab

by

CEN-Saclay, LAPP-Annecy, INFN-Trieste,
Kyoto University, Kyoto-Sangyo University, Kyoto University of Education,
Hiroshima University, University of O.E.H. (Kita-Kyushu),
Argonne National Laboratory, Fermi National Accelerator Laboratory,
University of Iowa, Los Alamos National Laboratory,
Northwestern University, Rice University, IHEP-Serpukhov,
University of Udine Collaboration*

31 March 1989

Preface

Part of P-678 was included in E-704 following the PAC's recommendations in 1981. In E-704, we explore a relatively lower region of $p_\perp$ in the π^0 production. On March 8, 1989, there was a meeting with the Fermilab management to discuss the status of the electromagnetic calorimeter for the polarized-beam experiments. During the meeting it was suggested that we update P-678 before the April PAC meeting. Although studies on the single-gamma measurements are continuing, we consider this P-678 update to be reasonably adequate. We are also counting on learning many facts about π^0 detection, which relates to direct-gamma detection, during the forthcoming E-704 run.

---

* Individual names are likely to be similar to the present participants in E-704. Precise list will be presented later.

Scientific Spokesman: Sergei Nurushev, IHEP - Serpukhov
Deputy Spokesman: K. Kuroda, LAPP - Annecy

ABSTRACT

We propose to measure the single-spin asymmetry parameter A_N in inclusive π° production at high $p_\perp$ and direct-γ production using the polarized proton-beam facility at Fermilab. In addition, we propose to measure the double-spin asymmetry parameter A_{LL} in inclusive π° production and direct-γ production using a polarized ^{6}LiD target.

A number of lead-glass counters will be doubled compared with existing E-704 electromagnetic calorimeter in order to gain rate and improve misidentification problems.

I. Introduction

Asymmetry measurements in π° production yield a value as large as A_N = 60% in the $2 < p_\perp < 3$ GeV/c region measured at 24 GeV/c (CERN) and 40 GeV/c (Serpukhov).[1] It seems important to pursue measurements to higher values of $p_\perp$ in order to investigate the spin dependence in the hard scattering of hadronic constituents. Simultaneously, the asymmetry in direct-γ production can be measured where $A_N = 0$ is expected by QCD perturbative theory.

Results of new measurements by the EMC group at CERN have been interpreted to mean that the proton spin may not be due to the helicity of its constituent quarks. Most of the proton spin may be due to gluons and/or orbital angular momentum. To understand the basic question of the origin of proton spin, π° and direct-γ production measurements at high $p_\perp$ with longitudinally polarized protons on longitudinally polarized target protons seem to be very desirable.[1]

The QCD Compton effect, gluon + quark → gamma + quark, is expected to be the dominant mechanism for direct-γ production at large $p_\perp$. In contrast to the π°, which represents only a fragment of the scattered constituent, the γ

itself participates directly in the hard-scattering process. As a direct consequence the ratio γ/π° should increase with increasing $p_\perp$, this prediction has been confirmed in several different experiments.[3] Thus, direct-γ production provides a particularly clean process for studying the dynamics of hadronic constituents without the complexities of quark fragmentation.

Although important qualitative features may be deduced from single-spin asymmetry measurements, the study of double-spin asymmetries can provide quantitative insight into the spin properties of gluons which are not accessible to deep-inelastic ep scattering experiments. The double-spin asymmetry A_{LL} in inclusive π° and direct-γ production has been estimated by several authors.[2,4]

We propose to study spin dependence in the reactions

$$p + p \rightarrow \pi^\circ + \text{anything}, \tag{1}$$

and

$$p + p \rightarrow \gamma + \text{anything} \tag{2}$$

with emphasis on the high-$p_\perp$ region (up to 6 GeV/c). The quantities to be measured are the single-spin asymmetries

$$A_N = \frac{Ed^3\sigma(\uparrow)/dp^3 - Ed^3\sigma(\downarrow)/dp^3}{Ed^3\sigma(\uparrow)/dp^3 + Ed^3\sigma(\downarrow)/dp^3} \tag{3}$$

for both reactions (1) and (2) with a transversely polarized proton beam and liquid hydrogen (H_2) target. In addition we propose to measure the double-spin asymmetry for (1) and (2).

$$A_{LL} = \frac{Ed^3\sigma(++)/dp^3 - Ed^3\sigma(+-)/dp^3}{Ed^3\sigma(++)/dp^3 + Ed^3\sigma(+-)/dp^3} \tag{4}$$

where ++(+-) indicate parallel (antiparallel) helicities for longitudinally polarized beam and target protons. This measurement requires replacement of the liquid H_2 target by a polarized ^6LiD target.

Major changes in this proposal from the E-704 setup are: i) doubled lead-glass counters, ii) polarized ^6LiD target, and iii) installation of guard counters surrounding the lead-glass counters.

II. Experimental Methods

A. Experimental Arrangement

A schematic view of the experimental arrangement is shown in Fig. 1. The polarized proton beam enters from the left. Trajectories of individual beam particles are defined by hodoscopes H_{B1} and H_{B2}; these are separated by 20 meters and have spatial resolutions of 1.5 mm in both the x and y directions. For single-spin measurements a liquid H_2 target 100-cm long will be used with the proton beam transversely polarized. For the double-spin asymmetry measurements the longitudinally polarized proton beam will be incident on a longitudinally polarized ^6LiD target. The proposed snake system will allow the beam polarization to be frequently flipped with no important change in beam geometry.

Photons from the decay of π°'s produced by the interaction of protons on either a LH_2 or polarized target are detected in the two Pb-glass calorimeters G_1 and G_2 (called "CEMC", central electromagnetic calorimeter) consisting of 2016 cells as shown in Fig. 1. The number of lead-glass in the present E-704 CEMC (1008 cells) will be doubled. At p_{in} = 200 GeV/c the CEMC is placed 10 m downstream of the target and centered around θ = 97 mrad which corresponds to x_F = 0. The azimuthal angle subtended by each calorimeter is $\pm$ 45° with respect to the horizontal plane.

The proportional chambers placed between the target and the CEMC serve to localize charged particles which accompany γ's and assure no charged tracks in the γ direction. To improve background identification in direct-γ production, the CEMC is provided with additional γ detectors G_1' and G_2' as shown in Fig. 1. These additional counters ensure identification of π° and η° decays in which only one γ falls within the fiducial area of the CEMC.

The acceptance of the detector in x_F-$p_\perp$ space in shown in Fig. 2 for p_{in} = 200 GeV/c.

B. Electromagnetic Calorimeters

The electromagnetic calorimeters (CEMC) comprise a major part of the detector. Each consists of 1008 Pb-glass cells (3.8 x 3.8 x 45 cm) stacked to form a trapezoidal array as shown in Fig. 3. The Cerenkov light is collected by a photomultiplier at the rear of each cell. (The detector elements and the design of the associated electronic system are similar to those developed by the IHEP-IFSN-LAPP Collaboration for the GAMS 4000 spectrometer at CERN.)

The principal characteristics of P-678 CEMC are listed in Table I. This detector has shown remarkable spatial resolution ($\pm$ 1 mm at 100 GeV), resulting from an optimal choice of tranverse dimensions of the Pb-glass cells.

To accommodate high event rates the integrated charge in each cell is digitized with its own ADC. Pedestal subtraction and energy normalization are performed automatically by a fast processor. Relative gains (PM + ADC) will be monitored with an LED system between spills. The energy resolution has been measured during the last fixed-target run; at full width half-maximum (FWHM) it is

$$\Delta E/E = 0.024 + 0.12/\sqrt{E}\ (\mathrm{GeV})$$

giving ± 2.5% at 25 GeV. Linearity has been studied with electrons from 30 to 40 GeV, and no deviation larger than 1% was observed.

Energies and coordinates (using the method of moments) will be evaluated on-line. This provides the possibility for on-line calculation of gamma-gamma invariant mass and kinematics, and allows one to impose event selection criteria if necessary before recording data on tape. With reasonable estimates for processing times we conclude that as many as 500 events/sec can be recorded even with large multiplicities.

C. Identification of π° Events

It is apparent, however, that event rejection is preferably executed off-line after careful study so that no bias is introduced in the inclusive final states.

To obtain a 'clean' sample of π° events all data must be subjected to extensive off-line analysis. Backgrounds due to improperly paired γ's will be estimated using the LUND Monte Carlo (PYTHIA) simulation. Contamination of the final sample by π°'s from decay of inclusively produced η's, ω°'s, and K_s°'s can be reasonably estimated from available measurements and LUND Monte Carlo calculations which relate charged and neutral production. This contamination will be small at high $p_\perp$.

D. Identification of Direct-γ Events

The problems involved in identification of direct-γ's in a background of π° decays have recently been addressed with considerable success.[3] Background arises from

i) The decays $\pi^\circ \to \gamma\gamma$ and $\eta \to \gamma\gamma$ in which one γ misses a spectrometer, is below threshold for detection, converts in the target, or the two γ's are too closely spaced to be geometrically resolved.

ii) We assumed that a background of η decays is negligible compared with π° based on the UA6 experiment.[3] Additional comments are made on page 9.

iii) Neutral hadrons such as n, $\bar{n}$, or K_L° which interact in the Pb-glass and a simulate a single shower.

In order to see the feasibility of the high-$p_\perp$ single-γ measurements, two cases (see a and b below) of fake single γ sources, and the single-gamma detection efficiency (see c) have been studied by Monte Carlo simulation. A coarse calorimeter surrounding the CEMC is discussed (see d). π° conversions in the polarized target is estimated (see e).

a) Two γ's from a π° are misidentified with a single energy cluster on the calorimeter even though both γ's hit the CEMC.

The CEMC is placed at z = 1000 cm as above. The electromagnetic showers were generated using the GEANT3 software package. The energy clusters in the CEMC were reconstructed using software developed by the Serpukhov group. The reconstruction was made with a certain energy threshold for each energy cluster, because we would have to set such an energy threshold in the off-line analysis for the real events in order to avoid noise signals. If two γ's are too close in space (e.g. as close as 3 cm at $p_\perp$ = 5.5 GeV/c), then the present reconstruction program tends to fail to divide the energy properly between two γ's. The mass reconstruction becomes worse in such cases. However, the program can tell whether the shower consists of a single-γ or multiple-γs with a minimum of two γ separation of $\sim$ 2cm by checking the shower shape. One ADC channel corresponds to 0.02 GeV, and we expect the noise level to be about 0.1 GeV or less. The ratio of this type of fake single γ's over π°'s is estimated to be below 1.7% throughout the $p_\perp$ range from 2.5 to 5.5 GeV/c. This is lower than the direct-γ production rate.

b) One γ from a π° hits the CEMC with high-$p_\perp$ and the other misses the lead-glass.

The background events in which one γ from a π° hits the CEMC with high-$p_\perp$ and the other γ misses the CEMC can be reduced by placing a surrounding coarse calorimeter around the CEMC. Figure 4 shows the fraction of π° events for which a gamma is missed and found in the surrounding calorimeter. The γ's hitting the surrounding calorimeter have low energies; about 30% of such γ's have an energy less than 0.6 GeV, because the γ's hitting the CEMC have to carry much larger fractions of the parent π° energies to clear the $p_\perp$-threshold.

Figure 5 shows the resulting fake direct-gamma spectrum. This includes the fact that the remaining gamma is lower energy (and $p_\perp$) than the π°, giving approximately an additional order of magnitude suppression in rate at a given $p_\perp$. The resulting background is about 1% of the π° rate at a given $p_\perp$. It also includes loss of one gamma due to conversions in the target material as mentioned in point e.

Therefore, it is nice to have the surrounding calorimeter as illustrated in Fig. 4 but not absolutely necessary.

Preliminary studies for similar problems due to missing one gamma from η decays have been done. These indicate no serious problem above $p_\perp$ of 1.5 GeV/c.

c) Direct photon and accompanying photon(s)

Multiple γ's entering the CEMC with real single-γ events are estimated to be about 10% of real events. Figure 6 shows the probability of direct photon without accompanying photon(s) in either the CEMC or the surrounding calorimeter estimated by the LUND (PYTHIA) Monte Carlo.

d) Coarse electromagnetic calorimeters G_1' and G_2' surrounding the CEMC will likely be segmented lead-sandwiched scintillators. The detector is currently being designed.

e) Another source of single gamma background from conversions in the target

The target is about 26% of a radiation length and the vacuum shells about 4%. As discussed above, the remaining gamma is of lower energy than the π° and so the background spectrum is only 1% of the π° spectrum at a given $p_\perp$. This is included in Fig. 5.

The neutral hadron contribution to background will be measured in a separate run using the method of Cox et al.[5] Ten radiation lengths of Pb will be inserted in the space between the proportional chambers and the Pb-glass spectrometers. The γ flux is largely degraded while the neutral hadronic component is attenuated only 30% due to interactions in the Pb. This background varies depending on the kinematic region and therefore must be subtracted separately in each X_F and $p_\perp$ interval.

The inclusive π°'s and direct-γ's will be carried out simultaneously for both A_N and A_{LL} measurements.

E. Polarized ^{6}LiD Target

It was recently established[6] that substantial nuclear polarizations can be achieved in large targets of ^{6}LiD. To the extent that $^6Li^\uparrow$ can be viewed as $\alpha + D^\uparrow$, fully one-half of the nucleons are polarized in such a material. Polarizations of $^6Li^\uparrow$ and $D^\uparrow$ approaching 70% should be achievable in the MP-9 polarized target, with the addition of a high-frequency (180 GHz) microwave source.

III. Rate and Error Estimate

Rates for π° and γ production have been estimated with the following assumptions:

Primary Beam: $4 \cdot 10^{12}$ incident protons/spill

Beam Momentum: 200 GeV/c

Beam Intensity: 3×10^7/spill with 1 spill/60 sec, and polarization $P_B = 0.45$

Geometrical Efficiency for π° detection = 0.25

Geometrical Efficiency for γ detection = 0.50

Liquid H_2 target: 100-cm long for A_N measurements

Polarized ^{6}LiD target ($\alpha + 2p^\uparrow + 2n^\uparrow$): 20-cm long for A_{LL} measurements

A) A_N Measurement

The invariant cross section for π° production was calculated with the parametrization of R. M. Baltrusaitis et al. [7]

$$f = E \frac{d^3\sigma}{d^3p} = A\, P_\perp^{-N} (1 - X_R)^M,$$

where $X_R = \sqrt{X_F^2 + X_\perp^2}$, $A = 3.12 \times 10^{-27}$ cm^2/GeV^2, $M = 4.81$, $N = 8.9$. The results are given in Table 2 for an integrated beam intensity of 1.8×10^{12} polarized protons corresponding to 1000 hours running time.

The statistical error in A_N is

$$\Delta A_N \approx \frac{\sqrt{\chi}}{P_B} \frac{1}{\sqrt{N_{Tot}}},$$

where $\chi = 1 + \frac{B}{S}$ and B/S = background over signal ratio.

In this case the backgrounds result largely from pairs of uncorrelated γ's which fall within the π°-acceptance criteria. This background can be estimated from the 2γ effective-mass distributions. With $\chi = 1.1$ as a reasonable estimate we obtain the errors ΔA_N given in Table II.

A similar estimate has been made for ΔA_N in direct-γ production. In this case it was assumed that the ratio γ/π° varied from 1/20 at $p_\perp = 3$ GeV/c to 1/10 at $p_\perp = 5$ GeV/c. With the assumption $\chi \simeq 1.5$ we obtain the estimated statistical errors given in Table III.

B) A_{LL} Measurement

The double-spin asymmetry measurements require both polarized beam and target. The statistical error may be approximated

$$\Delta A_{LL} \simeq \frac{\sqrt{\chi}\,\alpha}{P_B P_T} \frac{1}{\sqrt{N_{Tot}}}$$

here the 'polarization dilution factor' α reflects production on unpolarized target constituents. This factor depends not only on the target material but also on the kinematic conditions, particularly $p_\perp$. To estimate ΔA_{LL} we assumed that $\alpha \approx 2$ to 3 as $p_\perp$ increases from 2-5 GeV/c. For the double-spin asymmetry we obtain the errors ΔA_{LL} given in Tables IV and V for $pp \to \pi^\circ X$ and $pp \to \gamma X$, respectively.

SYSTEMATIC ERRORS:

The systematic errors divide roughly into multiplicative and additive. Uncertainties in target and beam polarizations are multiplicative errors. Target polarization can be measured to $\pm$ 3% with the principal uncertainty in calibration of the nuclear magnetic resonance system which uses the thermal equilibrium signal. It is estimated that beam polarization can be calculated to $\pm$ 3% from the beam optics.

Additive errors which may introduce a spurious asymmetry in the data can arise from

i) changes in beam geometry with reversal of beam polarization

ii) misalignment of detector components

iii) changes in gain of spectrometer elements.

Geometric sources of error associated with either the beam or detector can be accurately controlled through frequent cross-checks of counting rates with different spin-spin and spin-detector (right or left) combinations. With frequent reversals of beam polarization long-term variations in gain will be averaged out.

IV) Beam Time Request

1) 250 hours for beam polarization studies by polarimeters

2) 250 hours for lead-glass calibration

3) 1000 hours for $A_N(p^{\uparrow}p \rightarrow \pi^{\circ}X)$ and $A_N(p^{\uparrow}p \rightarrow \gamma X)$

4) 1000 hours for $A_{LL}(p^{\uparrow}p^{\uparrow} \rightarrow \pi^{\circ}\ X)$ and $A_{LL}(p^{\uparrow}p \rightarrow \gamma X)$

We will be ready to carry out these measurements during the next-fixed target period (not forthcoming) and likely before E-704 follow up (two-spin hyperon production measurement, to be specified).

V) Additional Equipment Needs Beyond E-704

Lead-glass counters, phototubes and bases	Serpukhov
Electronics, mainly fast bus ADC and H.V. power supplies (60K + 100K)	Argonne and Fermilab
^{6}LiD target	Argonne, Saclay, Los Alamos
Gamma detector surrounding the CEMC	Shared by collaboration
Cables and connectors (signal and H.V.)	Fermilab

VI Special Remarks

Energy Upgrade

We would like to point out the importance of the MP-beam energy upgrade. In general, we would like to investigate the energy dependence of various reactions studied in E-704 from 200 to 500 GeV/c. We specifically describe the advantages at higher energies concerning this proposal.

i) Direct-gamma production cross section at high $p_\perp$ increases rapidly with energy; from 200 to 500 there is more than a one-order increase. This will allow us to cover higher $p_\perp$ region.

ii) For the study of gluon spin distribution, we need to cover low $X_\perp$ region ($X_\perp = 2p_\perp/\sqrt{s}$) at high $p_\perp$ and high s. We can reach $X_\perp$ = 0.3 (at $p_\perp$ = 5 GeV) at 500 GeV.

Polarized ^{7}LiH Target

We plan to propose a similar measurement with a polarized ^{7}LiH target to investigate possible differences in effect due to polarized proton and polarized neutron.

REFERENCES

1) A. N. Vasiliev, Proceedings of the Symposium on High Energy Spin Physics, Minneapolis, Minnesota, September, 1988.

2) This topic was extensively described during the Fermilab Polarization Symposium, June 1988 (See Proceedings of the Symposium on Future Polarization Physics at Fermilab); S. Brodsky et al., Phys. Lett. (1988); E. L. Berger and J. Qiu, to be published.

3) For instance, see A. Bernasconi et al., Phys. Lett. 206, 163 (1988); T. Ferbel and W. R. Molzen, Rev. of Mod. Phys. 56, No. 2, Part 1, 181 (1984).

4) M. B. Einhorn and J. Soffer, Nucl. Phys. 274, 714 (1986); N. S. Craigie, K. Hidaka, M. Jacob, and F. M. Renard, Phys. Reports, 99, 143 (1983), and references therein.

5) B. Cox et al., Proc. 1979 Int. Symp. on Lepton and Photon Interactions at High Energies, Fermilab, Batavia, p. 602.

6) P. Chaumette et al., Proceedings of the Symposium on High Energy Spin Physics, Minneapolis, Minnesota, September, 1988.

7) R. M. Baltrusaitis et al., Phys. Rev. Lett. 44, 122 (1980).

8) K. Hidaka, private communication.

9) M. J. Alguard et al., Phys. Rev. Lett. 37, 1261 (1976); 41, 70 (1978); G. Baum et al., Phys. Rev. Lett. 51, 1135 (1983).

10) J. Ashman et al., (European Muon Collaboration), Phys. Lett. B206, 364 (1988).

APPENDIX

A_{LL} Measurement and Gluon Spin Distribution

We describe here how to determine the gluon polarization by measuring the parameter A_{LL} in direct-gamma production, $p^{\uparrow}p^{\uparrow} \rightarrow \gamma + X$ (a polarized beam on a polarized-proton target).

To good approximations for $x_{\perp} \gtrsim 0.1$,[4]

$$A_{LL}\ (x_F = 0,\ x_{\perp}) \simeq [\Delta U(X_{\perp})/U(X_{\perp})] \cdot [\Delta V(X_{\perp})/V(X_{\perp})] \cdot \hat{A}_{LL}^{UV}\ (\hat{\theta}_{c.m.} = 90^0),$$

where, $\Delta U/U$ represents U quark polarization, $\Delta V/V$ gluon polarization, and $\hat{A}_{LL}^{UV}$ in $U^{\uparrow}V^{\uparrow} \rightarrow U\gamma$ at $\hat{\theta}_{c.m.} = 90^0$.

One can relate[8] $\Delta U(X_{\perp})/U(X_{\perp})$, which can be obtained from A_1 values.[9,10]

$$\hat{A}_{LL}^{UV}\ (\hat{\theta}_{c.m.} = 90^0) = +\ 0.6 \text{ by QCD.}$$

Thus, we will be able to determine $\Delta V(X_{\perp})/V(X_{\perp})$ by measuring $A_{LL}\ (x_F = 0,\ X_{\perp})$.

Table I

Parameters and Characteristics of the CEMC

-	Lead-glass cell dimensions	38 x 38 x 450 mm^3
-	Type of glass	F-8
-	Total number of cells	2016
-	Working area and weight of the spectrometer	$0.8m^2$, 2.5 t
-	Photomultiplier	FEU-84-3
-	Accuracy in measuring photon coordinate	
	At 25 GeV	± 2 mm
	At 100 GeV	± 1 mm
-	Photon energy resolution	
	At 25 GeV	± 2.5%
	At 100 GeV	± 1.5%
-	Mass resolution for decaying particles	± 8%
-	Time resolution	40 nsec gate

Table II

Estimates of Total Number of Events and Corresponding Statistical Errors

In A_N ($pp \rightarrow \pi^\circ x$) for 1000 Hours Use of the Beam Time

$p_\perp$ (GeV/c)	$x_\perp$	Δx_F	$\Delta p_\perp$	Number of Events	ΔA_N %
2 - 2.5	0.21	0.1	0.5	7.2×10^6	0.10
2.5 - 3	0.26	0.1	0.5	1.1×10^6	0.24
3 - 4	0.31	0.125	1.0	2.6×10^5	0.45
4 - 5	0.41	0.15	1.0	1.4×10^4	2.0
5 - 6	0.52	0.20	1.0	9.3×10^2	8.1

Table III

Estimates of Total Number of Events and Corresponding Statistical Errors

In A_N ($pp \rightarrow \gamma x$) for 1000 Hours Use of the Beam Time

$p_\perp$ (GeV/c)	$x_\perp$	Δx_F	$\Delta p_\perp$	Number of Events	ΔA_N %
2 - 2.5	0.21	0.1	0.5	3.6×10^5	0.35
2.5 - 3	0.26	0.1	0.5	5.5×10^4	1.4
3 - 4	0.31	0.125	1.0	1.3×10^4	2.0
4 - 5	0.41	0.15	1.0	1.4×10^3	7.5

Table IV

Estimates of Statistical Errors in A_{LL} (pp → π^0x) Assuming 1000-Hour Use of the Beam Time

$p_\perp$ (GeV/c)	$\Delta p_\perp$	Number of Events	ΔA_{LL}%
2.0 - 2.5	0.5	$1.6 \cdot 10^7$	0.15
2.5 - 3.0	0.5	$2.3 \cdot 10^6$	0.40
3.0 - 4.0	1.0	$5.5 \cdot 10^5$	1.0
4.0 - 5.0	1.0	$3.0 \cdot 10^4$	4.0

Table V

Estimates of Statistical Errors in A_{LL} (pp → γx) Assuming 1000-Hour Use of the Beam Time

$p_\perp$ (GeV/c)	$\Delta p_\perp$	n	ΔA_{LL}%
2.0 - 2.5	0.5	$8.0 \cdot 10^5$	0.8
2.5 - 3.0	0.5	$1.1 \cdot 10^5$	2.7
3.0 - 4.0	1.0	$2.8 \cdot 10^4$	4.0
4.0 - 5.0	1.0	$3.0 \cdot 10^3$	12

Figure Captions

Figure 1 Schematic view of the experimental arrangement.

Figure 2 x_F - $p_\perp$ coverage.

Figure 3 Lead-glass array in the CEMC.

Figure 4 The fraction of π°'s for which one gamma misses the lead glass but is not caught in surrounding coarse calorimeters. These curves can be extrapolated to the case of no surrounding counters. (This simulation was done for the CEMC consisting of 1008 cells.)

Figure 5 The fake direct gamma spectrum resulting from loss of one gamma from π° decay due to both geometrical acceptance and conversions in the target. No outer coarse calorimeter was assumed. (This simulation was done for the CEMC consisting of 2016 cells.)

Figure 6 Probability of direct-photon detection without accompanying photon(s) in either the CEMC or surrounding calorimeter (G_1' and G_2').

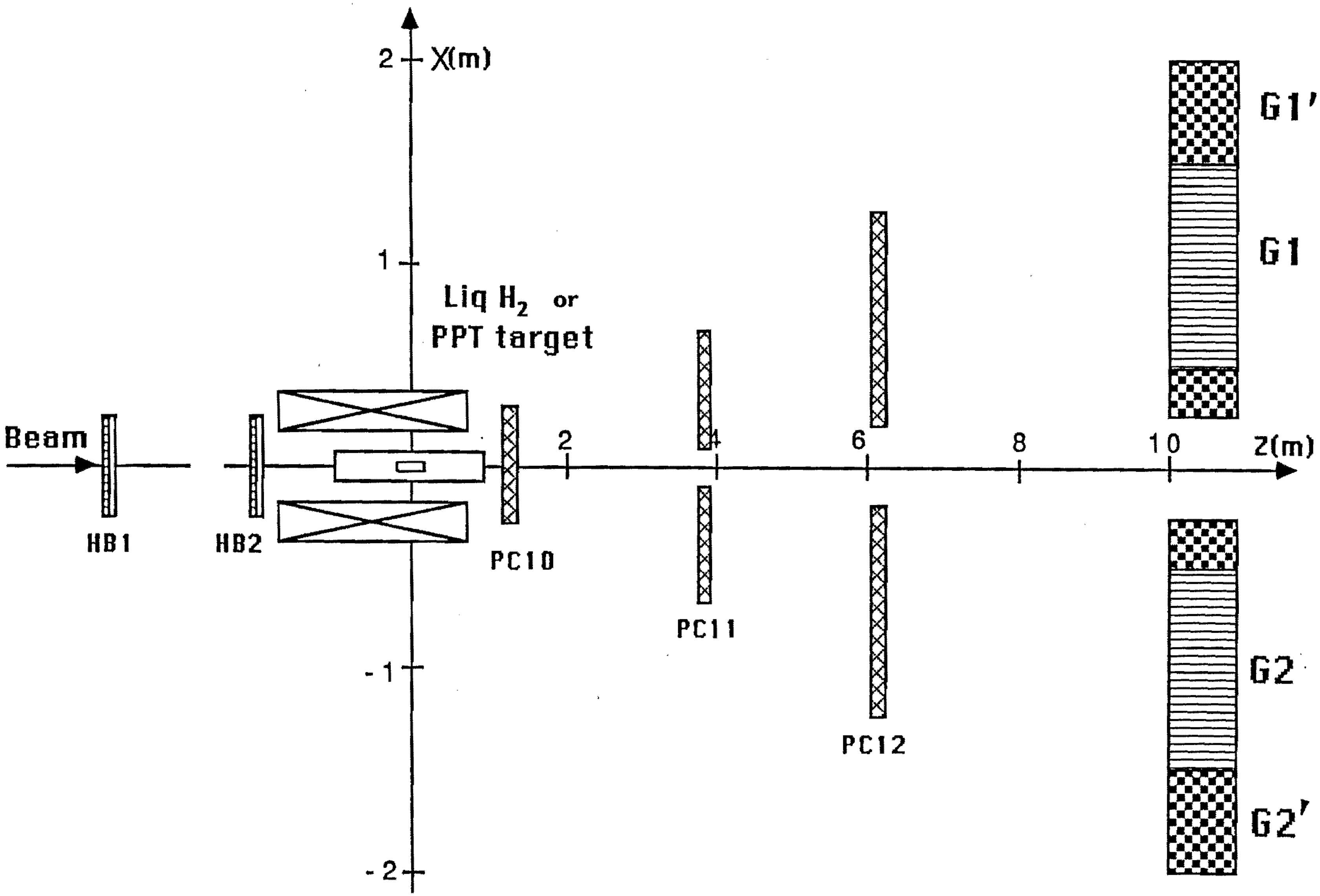

X(m)
2
1
-1
-2
Liq H_2 or
PPT target
Beam
HB1
HB2
PC10
PC11
PC12
2
4
6
8
10
Z(m)
G1'
G1
G2
G2'

FIGURE 1

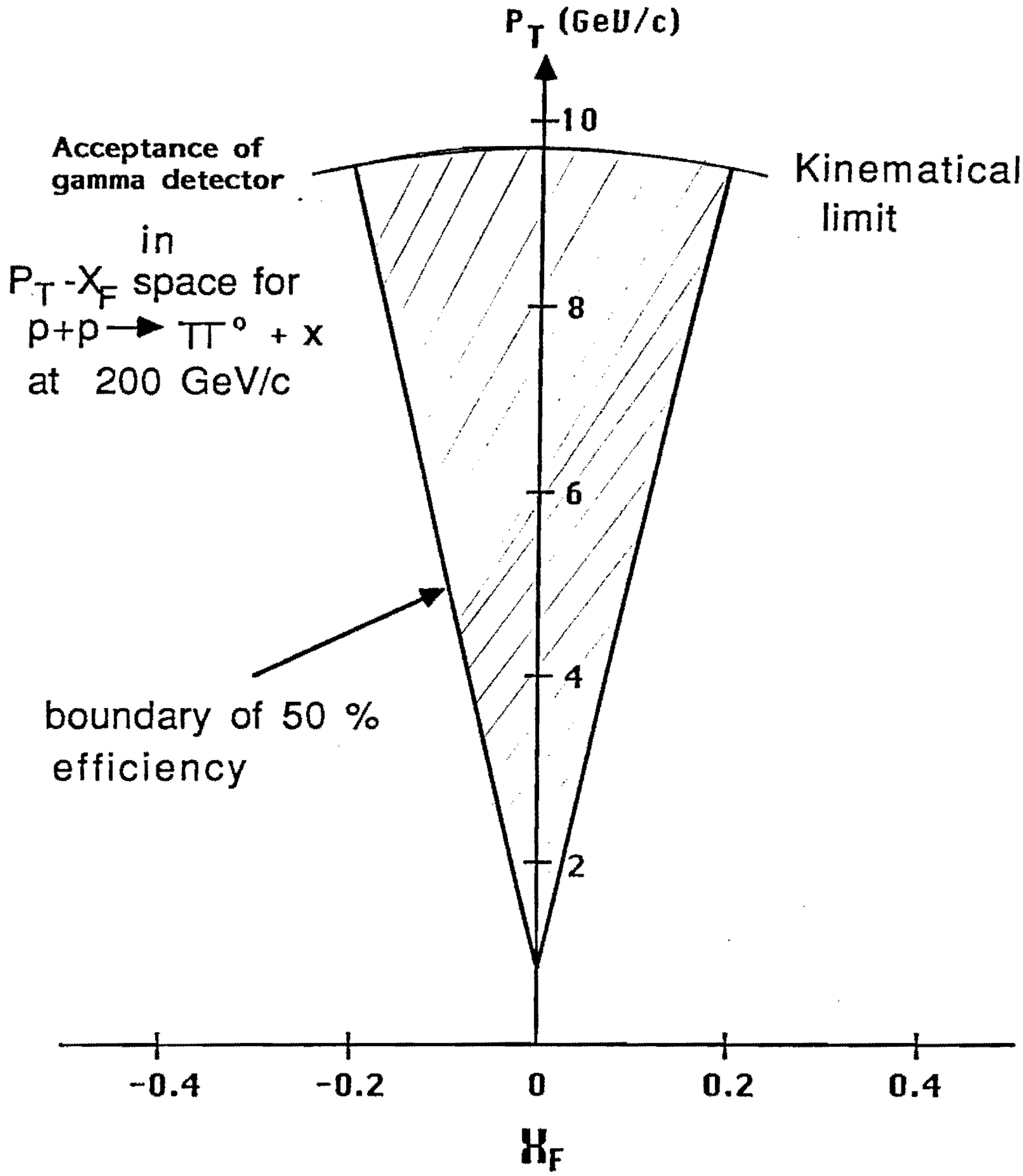

P_T (GeV/c)
10
8
6
4
2
Acceptance of
gamma detector
in
P_T -X_F space for
p+p → π° + x
at 200 GeV/c
Kinematical
limit
boundary of 50 %
efficiency
-0.4
-0.2
0
0.2
0.4
X_F

FIGURE 2

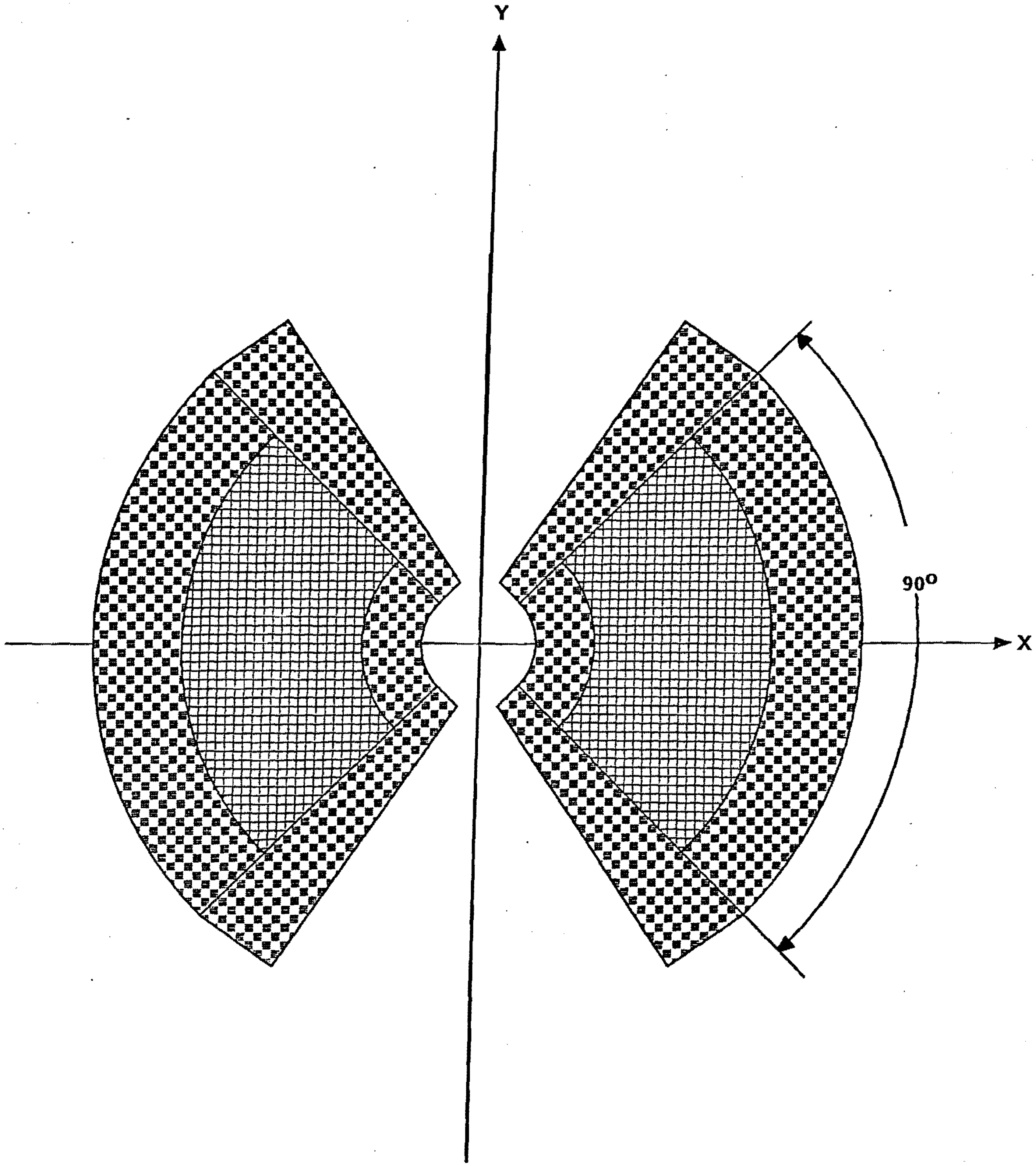

FIGURE 3

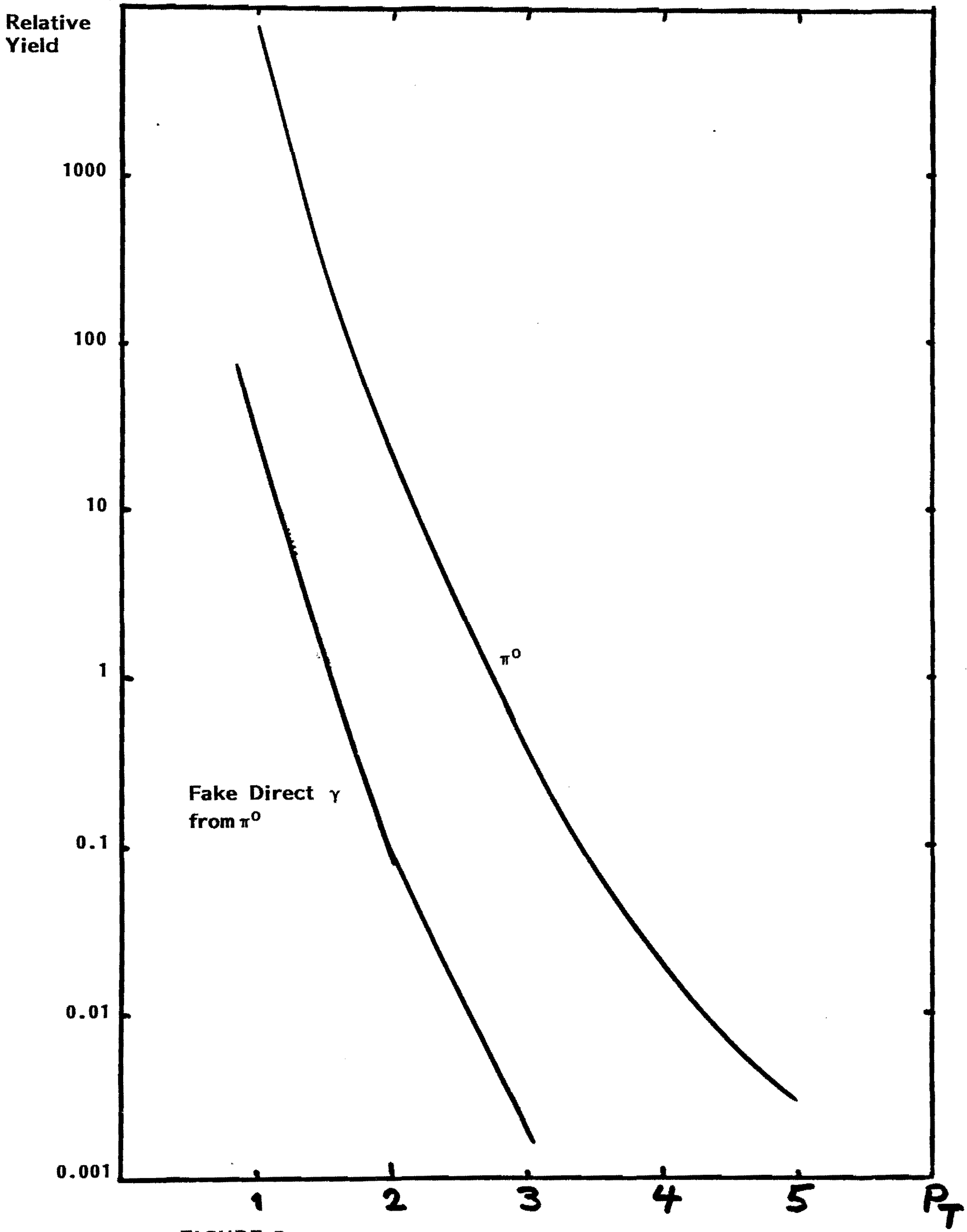
Relative Yield
1000
100
10
1
0.1
0.01
0.001
π^0
Fake Direct γ from π^0
1
2
3
4
5
P_T

FIGURE 5

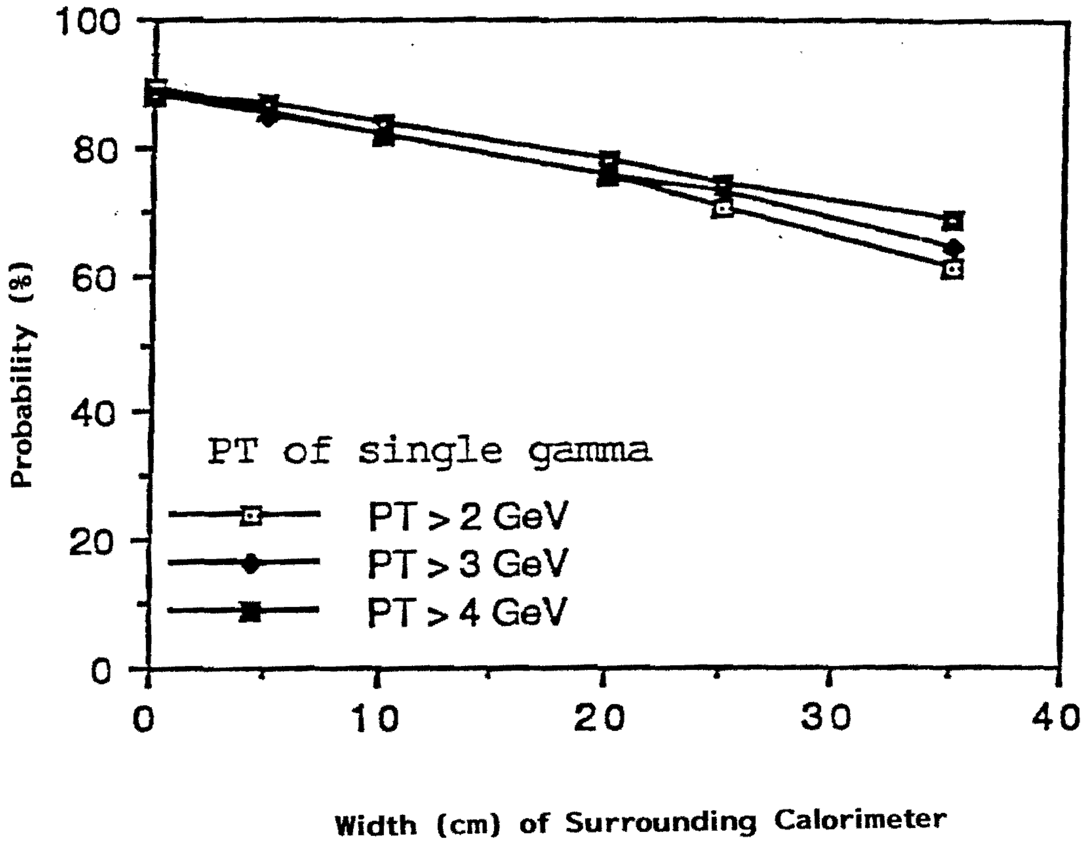
100
80
60
40
20
0
Probability (%)
PT of single gamma
PT > 2 GeV
PT > 3 GeV
PT > 4 GeV
0
10
20
30
40
Width (cm) of Surrounding Calorimeter

FIGURE 6